Technical Note

Transitional and Weir Flow in a Vented Drop Shaft with a Sharp-Edged Intake

Roberta Padulano, Ph.D.[1]; and Giuseppe Del Giudice, M.ASCE[2]

Abstract: An experimental analysis of a vertical drop shaft with a sharp-edged horizontal intake section and a coaxial venting pipe is undertaken to obtain design criteria given the limited attention provided by literature. Three different flow regimes are observed, namely weir flow and pressurized flow for extreme discharges and transitional flow for intermediate discharges. Particular attention is paid to transitional flow, which is a periodical regime consisting of an alternate switch from weir to pressurized flow, with water heads ranging between a maximum and a minimum. For transitional flow a detailed characterization of water surface oscillations is provided, and nondimensional equations are given describing mean water head, oscillation amplitude and frequency as functions of pipe Froude number and dimensionless plunged length of the coaxial pipe. Also, a region of existence is provided in terms of pipe Froude number and different wave types are identified. For weir flow, a nondimensional head-discharge relation is provided by analogy with overfalls. **DOI: 10.1061/(ASCE)IR.1943-4774.0001011.** *© 2016 American Society of Civil Engineers.*

Author keywords: Coaxial pipe; Drop shaft; Pressurized flow; Transitional flow; Venting system; Weir flow.

Introduction

Vertical drop shafts are often used in storm water sewer systems located in hilly regions to overcome significant elevation differences (Hager 2010). When designing a sewer system, professionals will refer to well-known drop shafts such as the morning glory type (Williams 1997; USBR 1987) or the vortex type (Del Giudice et al. 2010; Del Giudice and Gisonni 2011). However, when rehabilitating and retrofitting an existing drainage network, engineers must use already built facilities, if compatible with the expected discharges, to minimize costs. This often implies that the governing parameters and laws of rarely used hydraulic structures should be known.

The particular drop shaft which is the object of this research is very common within the sewer network of Naples City (Italy). Such a structure is used at present, although its hydraulic behavior is substantially unknown. In technical literature no information is available specifically related to a vertical drop shaft with a horizontal, sharp-edged circular intake; however, some information can be deduced about its hydraulic behavior from some experimental research regarding similar structures (Anwar 1965; Anderson et al. 1971; Khatsuria 2005; Padulano et al. 2013, 2015; Banisoltan et al. 2015). Because of such a lack of information, an experimental campaign was undertaken to identify hydraulic behavior and design criteria for this drop shaft that led to the definition of three different flow regimes for different discharge ranges (Padulano et al. 2013, 2015). Design equations were provided for pressurized flow for both cases of vented and unvented conditions; in the mentioned papers, venting was ensured by a coaxial circular pipe with diameter d, plunged within the drop shaft for a length nD, with n an integer number and D the diameter of the drop shaft. The advantages of considering a venting pipe were described in Padulano et al. (2013) for pressurized flow. The following dimensionless parameters were considered: (1) dimensionless water head $Y = h/D_{\mathrm{eq}}$; (2) dimensionless pressurized length $\lambda = L_p/D_{\mathrm{eq}}$; and (3) pipe Froude number $\mathsf{F}_D = Q/\sqrt{gD_{\mathrm{eq}}^5}$ (Hager and Del Giudice 1998). In these parameters D_{eq} is the equivalent diameter equal to $\sqrt{D^2 - d^2}$, which expresses the cross-section extent with and without the venting pipe, and L_p is the pressurized length which is equal to the entire length L of the drop shaft without venting pipe, whereas it is equal to the plunged length of the venting pipe nD when it is present.

In this paper, similar head-discharge relations are sought for transitional flow and weir flow for a vented vertical drop shaft with a circular sharp-edged horizontal intake; at this aim, a detailed characterization of oscillations is needed for transitional flow. The experimental campaign, whose preliminary phase (pressurized flow) was described in Padulano et al. (2013, 2015), particularly addresses the influence of the venting pipe so that results are provided for vented conditions only.

Experimental Setup

The experimental model consisted of a prismatic Plexiglas tank with a $0.7 \times 2.07\ \mathrm{m}^2$ rectangular plan section 1.25 m high; a filtering wall divided it into two equal parts, namely a detention tank and a filling tank up and downstream of the filter, respectively. The vertical drop shaft, simulated by a vertical Plexiglas pipe, was attached to the bottom center of the filling tank with a sharp-edged horizontal inlet, and its outflow was in the atmosphere [Figs. 1(a and b)]. To ensure air venting, a vertical pipe was coaxially housed in the shaft by means of an iron bracket at the tank top and three screws at the plunging end of the venting pipe. Different diameters $D = 100$ and 70 mm for the drop shaft and $d = 70$, 50, and 30 mm for the venting pipe were used; also, three different lengths $L = 1.5$, 1, and

[1]Dipartimento di Ingegneria Civile, Edile e Ambientale (DICEA), Università degli Studi di Napoli Federico II, 80125 Napoli, Italy (corresponding author). E-mail: roberta.padulano@unina.it

[2]Professor, Dipartimento di Ingegneria Civile, Edile e Ambientale (DICEA), Università degli Studi di Napoli Federico II, 80125 Napoli, Italy. E-mail: delgiudi@unina.it

Note. This manuscript was submitted on June 16, 2015; approved on December 7, 2015; published online on February 16, 2016. Discussion period open until July 16, 2016; separate discussions must be submitted for individual papers. This technical note is part of the ***Journal of Irrigation and Drainage Engineering***, © ASCE, ISSN 0733-9437.

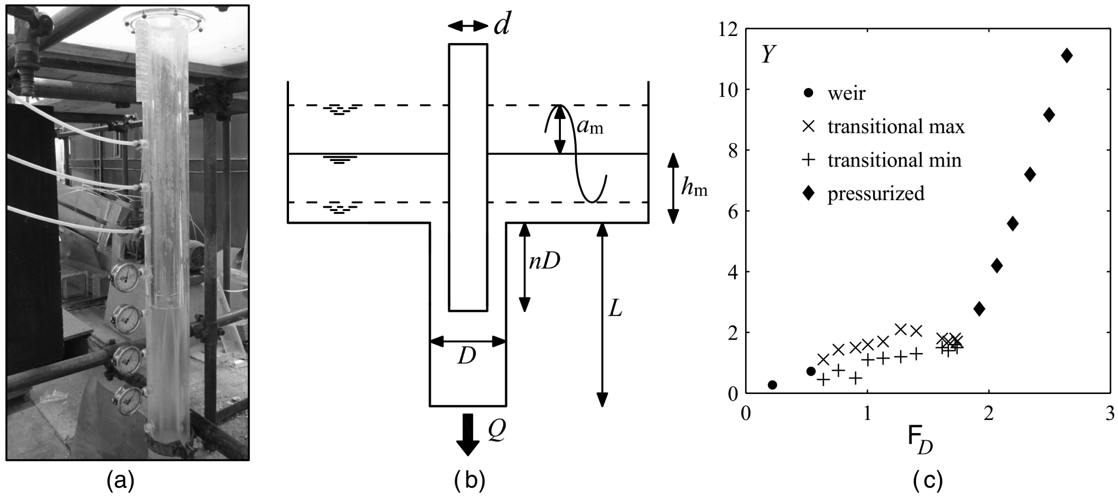

Fig. 1. (a) Experimental setup photograph; (b) sketch with governing variables; (c) typical head-discharge data

0.5 m were considered for the drop shaft. Discharges were measured along the supply line, upstream of the tank, by means of an orifice plate; the corresponding water level in the filling tank was evaluated by means of a point gauge with 0.5 mm accuracy. During transitional flow, a continuous monitoring was undertaken by means of a 25 frames per second camera.

Experiments were performed by varying the discharge and measuring the water head in the tank; both an emptying and a filling path were followed to verify whether any hysteretic behavior had occurred, yet without significant differences. The plunged length of the venting pipe was set equal to nD, with n being the plunging rate, set as an integer number varying between 2 and 9; 13 different configurations were investigated, each characterized by a different combination of the parameters D, d, L, and n.

Experimental Observations in Transitional Flow

Fig. 1(c) shows a typical experimental head-discharge relation where three different datasets can be observed corresponding to the three possible flow regimes: the two extreme datasets correspond to weir flow (lower extreme) and pressurized flow (upper extreme); in between two curves corresponding to the maximum and minimum values of water head describe the periodical oscillations typical of this regime. In transitional flow for fixed drop shaft and coaxial pipe diameters and lengths and for a fixed discharge the drop shaft switched between weir and pressurized flow conditions alternately with the water depth oscillating between a maximum and a minimum. Under the weir flow phase the water depth in the tank rose and a vena contracta occurred at the shaft intake, with the drop shaft occupied by air and water at atmospheric pressure. As the water depth gained its maximum the hydraulic regime shifted to a pressurized flow phase with the water depth plunging, and the drop shaft occupied by pressurized water with no visible vena contracta. Once the minimum was reached, weir flow phase was restored, generating a new cycle. This periodical oscillating behavior is highlighted in Fig. 2(a), where some examples of oscillations of water surface during transitional flow are shown.

Fig. 2(b) shows that for a fixed configuration, oscillations have different amplitude and frequency according to discharge. For increasing Froude numbers, namely for increasing discharge with a fixed configuration, the appearance of oscillations deeply changes with the pressurized phase (decreasing head) becoming more and more prevalent in time than the weir phase (increasing head). Three different wave profiles can be distinguished analyzing water head

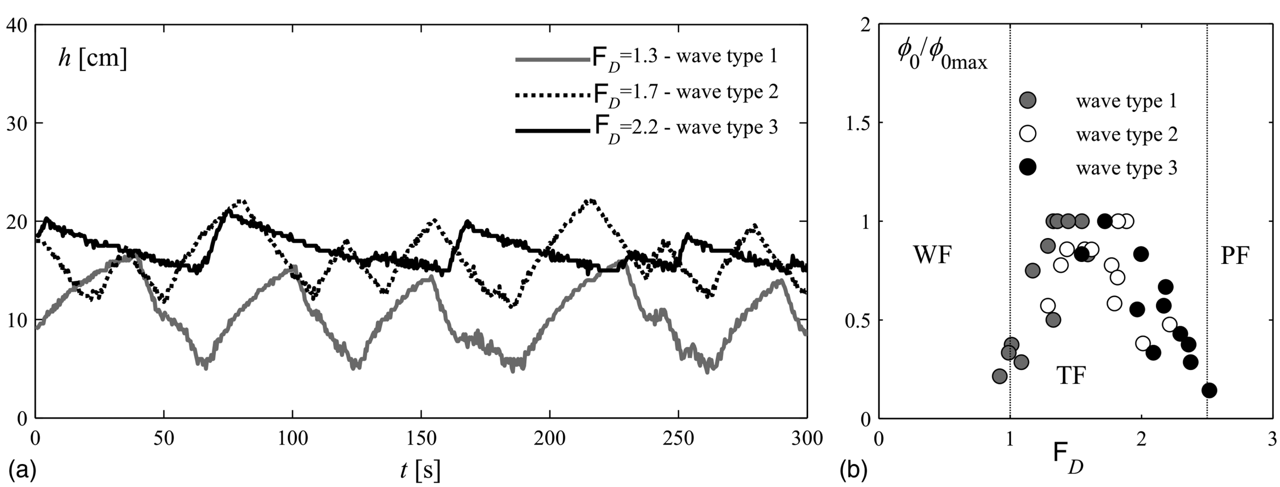

Fig. 2. (a) Wave profiles with varying F_D for a fixed configuration in transitional flow; (b) relation among oscillation frequencies, F_D, and wave types with flow sectors (WF = weir flow; TF = transitional flow; PF = pressurized flow)

time series [Figs. 2(a and b)]: Wave type 1 (predominance of weir phase), wave type 2 (similar duration of weir and pressurized phase), and wave type 3 (predominance of pressurized phase). Accordingly, oscillation frequency is lower for extreme discharges, whereas it is higher for intermediate discharges, namely when the recording time is equally occupied by weir phase and pressurized phase. Fig. 2(b) shows peak frequencies ϕ_0, which were extracted from each time series by means of a spectral analysis and related to the pipe Froude number F_D. Peak frequencies showed a parabolic behavior and had to be normalized by means of maximum frequency $\phi_{0\max}$ which proved to be a function of λ only. Please note that no oscillating behavior was observed for roughly $\mathsf{F}_D < 1$ and $\mathsf{F}_D > 2.5$; this range is similar to the one proposed by Banisoltan et al. (2015) referring to drill-drop manholes. The extremes of the proposed range are roughly set because when oscillation amplitudes reduce (because of the incoming evolution of transitional into either weir or pressurized flow), they can be confounded with the oscillations of water surface due to turbulence.

As concerns weir flow, no significant differences were observed among all configurations, both because of the small amount of data for this regime and because weir flow depends neither on the shaft length nor on the coaxial pipe plunging rate, but only on the perimeter dimensions and shape (Khatsuria 2005).

Experimental Results

Dimensional Analysis

A dimensional analysis was undertaken to understand about the significant dimensionless quantities governing flow. The phenomenon of interest can be described by a function G_1 of mean water head h_m (m), discharge Q ($m^3\,s^{-1}$), plunged length nD (m), equivalent diameter D_{eq} (m), gravity acceleration g ($m\,s^{-2}$), and oscillation amplitude a_m (m)

$$G_1(nD, D_{eq}, h_m, a_m, Q, g) = 0 \tag{1}$$

Choosing D_{eq} and g as scaling variables, Eq. (1) specifies in

$$G_2\left(\frac{nD}{D_{eq}}, \frac{h_m}{D_{eq}}, \frac{a_m}{D_{eq}}, \frac{Q}{\sqrt{gD_{eq}^5}}\right) = G_2(\lambda, Y_m, A_m, \mathsf{F}_D) = 0 \tag{2}$$

which gives the significant dimensionless numbers $Y = h_m/D_{eq}$, $\lambda = nD/D_{eq}$; $A_m = a_m/D_{eq}$; and $\mathsf{F}_D = Q/(gD_{eq}^5)^{1/2}$ (Hager and Del Giudice 1998; Padulano et al. 2013, 2015).

As concerns oscillation frequency ϕ, the Strouhal number was considered. Strouhal number S is defined as $\phi L/V$, being ϕ the frequency, L a characteristic length, and V the flow velocity; this dimensionless number is typically used when describing periodical flow patterns (Potter et al. 2011).

Transitional Flow

For this regime, fundamental oscillation characteristics are the mean water head h_m, the amplitude a_m (defined as the difference between a maximum or a minimum and h_m), and the frequency ϕ (defined as the reciprocal of the time distance between two consecutive maximum or minimum values).

As concerns h_m, a dimensionless mean water head was defined as $Y_m = h_m/D_{eq}$ based on dimensional analysis. Experimental evidence shows that Y_m is dependent on both the pipe Froude number and the dimensionless plunged length λ. Fig. 3(a) shows that Y_m increases with λ for a fixed F_D, and it increases with F_D for a fixed λ, namely for a given drop shaft geometry. The equation that best fits data is

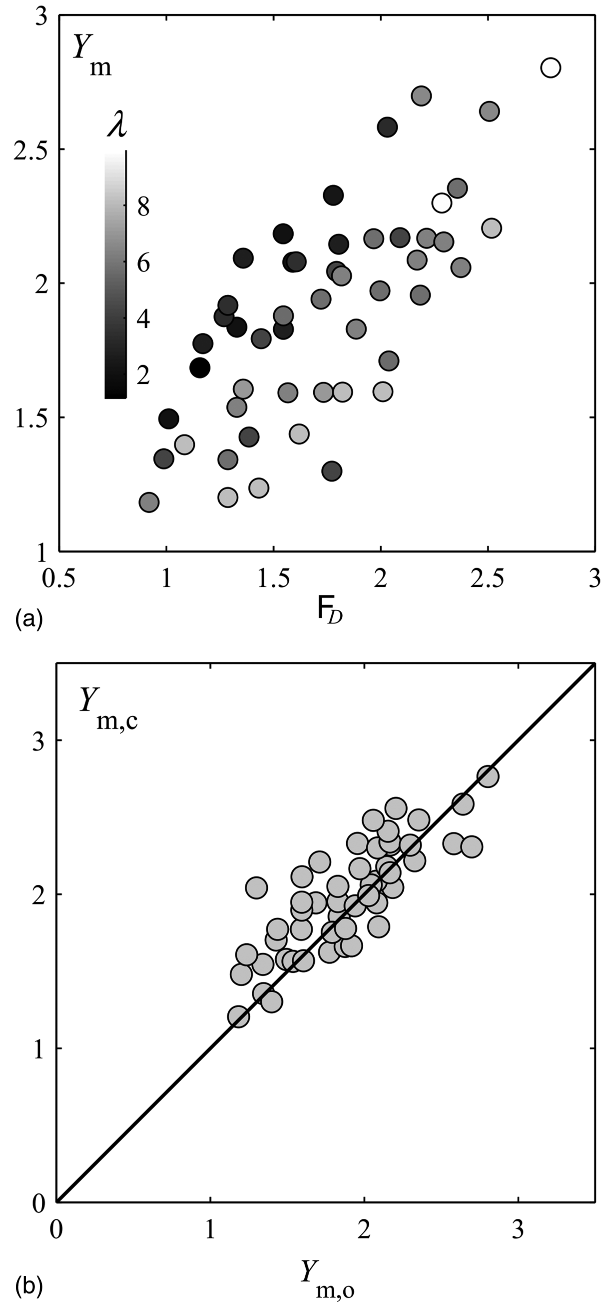

Fig. 3. (a) Relation between Y_m, F_D, and λ in transitional flow; (b) accordance between observed ("o") and computed ("c") Y_m with Eq. (3)

$$\mathsf{F}_D = 1.25 \cdot Y_m - \frac{1}{0.8 \cdot \sqrt{\lambda}} \tag{3}$$

Eq. (3) shows that, for a fixed Y_m, F_D increases with increasing λ with a square-root dependence, which is very close to the head-discharge relations for pressurized flow (Padulano et al. 2013, 2015). Fig. 3(b) shows the good accordance between observed Y_m values and those computed with Eq. (3).

Dimensional analysis defined the dimensionless mean oscillation amplitude as $A_m = a_m/D_{eq}$; however, experimental evidence showed that the parameter governing oscillations is $A^* = a_m/(nD)$ that implies $A^* = A_m/\lambda$. A^* decreases for increasing values of the product $Y_m \cdot \lambda$ by means of a power function [Fig. 4(a)]. Since Y_m depends on F_D and λ by means of Eq. (3), a relation was sought

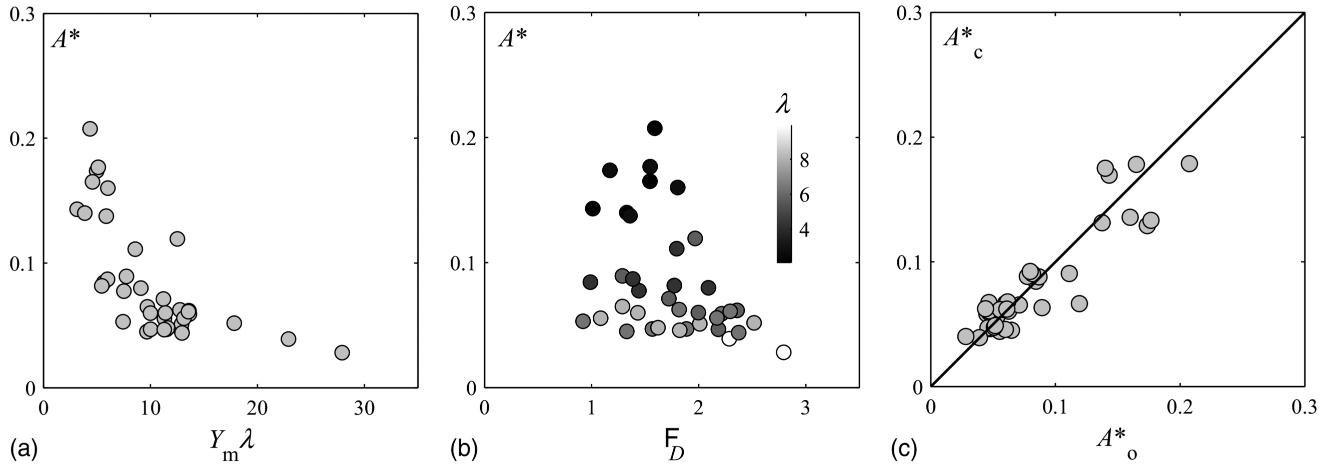

Fig. 4. (a) Dependence of A^* on product $\lambda^* Y_{\mathrm{m}}$; (b) relation among A^*, F_D, and λ; (c) accordance between observed ("o") and computed ("c") A^* with Eq. (4)

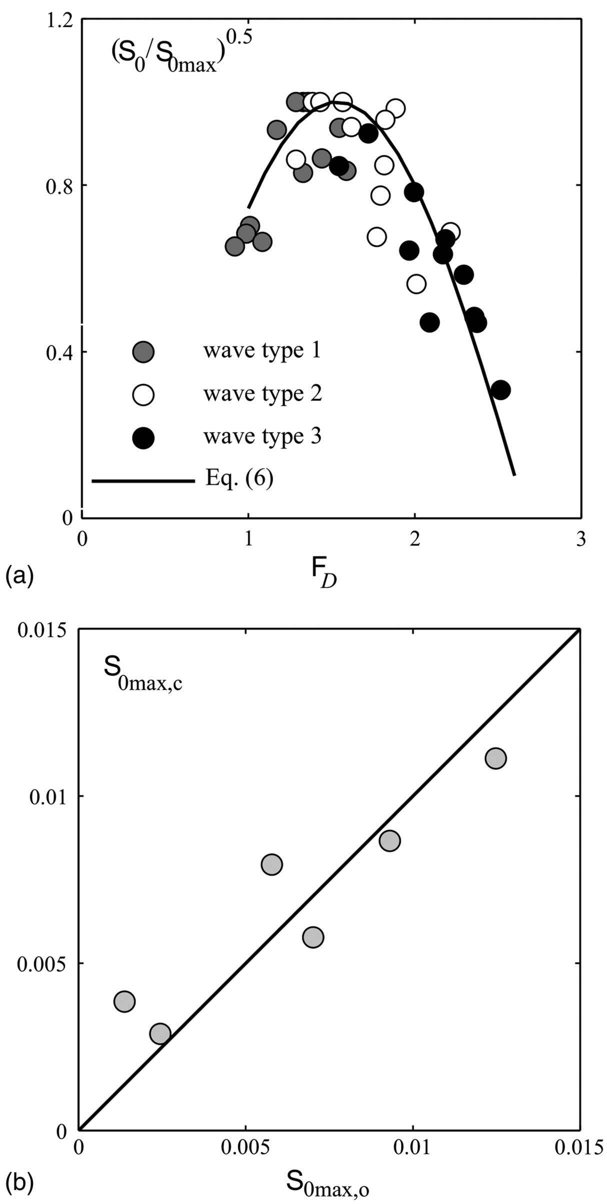

Fig. 5. (a) Relation among $\mathsf{S}_{0\max}$, F_D and wave type; (b) accordance between observed ("o") and computed ("c") $\mathsf{S}_{0\max}$ with Eq. (7)

among A^*, F_D, and λ on the basis of the dependences observed in Fig. 4(b), showing that A^* increases with increasing λ for a fixed F_D, whereas it is almost constant for a fixed λ. The equation that best fits data is

$$A^* = 0.35 \cdot \frac{\mathsf{F}_D^{0.12}}{\lambda} \tag{4}$$

Fig. 4(c) shows the good accordance between observed A^* values and those computed by means of Eq. (4).

As concerns oscillation frequencies, the Strouhal number S_0 referring to peak frequency is considered

$$\mathsf{S}_0 = \frac{\phi_0 nD}{V} = \frac{\pi}{4} \cdot \frac{\phi_0 nDD_{\mathrm{eq}}^2}{Q} \tag{5}$$

where the plunged length nD was chosen as characteristic length. $\mathsf{S}_{0\max}$ is the Strouhal number corresponding to maximum peak frequency $\phi_{0\max}$. Calibration of a periodical function $\mathsf{S}_0(\mathsf{F}_D)$ [Fig. 5(a)], resulted in

$$\sqrt{\frac{\mathsf{S}_0}{\mathsf{S}_{0\max}}} = \sin\left(\frac{2\pi \mathsf{F}_D}{4.6} - 0.5\right) \tag{6}$$

Eq. (6) shows that the square root of normalized peak Strouhal number is described by a sinusoid with period equal to 4.6 and phase equal to 0.5. Fig. 5(a) shows that Eq. (6) interpolates experimental data with good accordance. Fig. 5(a) also shows wave types, with wave type 2 occurring for maximum peak Strouhal numbers which correspond to intermediate F_D, whereas types 1 and 3 occur for the smallest and the highest F_D, respectively; this is consistent with Fig. 2(a). Finally, experimental evidence shows a linear dependence of $\mathsf{S}_{0\max}$ on dimensionless plunged length

$$\mathsf{S}_{0\max} = 0.0014 \cdot \lambda \tag{7}$$

Fig. 5(c) shows the good accordance between observed and calibrated $\mathsf{S}_{0\max}$. Eqs. (3), (4), (6), and (7) completely describe oscillations in transitional flow: For a fixed discharge and drop shaft configuration, Eq. (3) provides the mean water head, Eq. (4) provides oscillation amplitude (thus the maximum water head, which is an important design parameter), and the combined use of Eqs. (6) and (7) provide the oscillation frequency.

Weir Flow

For a vented drop shaft under weir flow conditions, each dimensionless discharge F_D corresponds to a unique dimensionless water head Y [Fig. 1(c)]; a simple data interpolation provides

$$\mathsf{F}_D = 0.544 \cdot Y^{3/2} \tag{8}$$

$\mathsf{F}_D = 1$ marks the passage between weir and transitional flow considerations about this passage value are reported in the "Experimental Observations in Transitional Flow" section. The exponent in Eq. (8) implies that $Q \sim h^{3/2}$ as suggested by Anwar (1965) and Khatsuria (2005). If Y and F_D in Eq. (8) are replaced with their definitions the head-discharge relation resembles a standard overfall head-discharge relation (Hager 2010) where discharge depends on the crest perimeter

$$Q = \mu \cdot \pi D_{\mathrm{eq}} \cdot h \cdot \sqrt{2gh} \tag{9}$$

with μ being the discharge coefficient for a double circular crest [Figs. 4(b and c)], which resulted equal to 0.1225. Consistently with overfalls hydraulics, no additional dependence was found on plunged length.

Conclusions

A detailed experimental analysis was undertaken concerning a vertical drop shaft with a sharp-edged horizontal intake and a coaxial circular venting pipe. The main purpose was to determine the performance and design criteria for this hydraulic structure under transitional and weir flow given the limited attention in technical literature.

Data allowed for the determination of the head-discharge relation for transitional flow [Eq. (3)] and weir flow [Eq. (8)]; these equations are valid for λ ranging between 2 and 10. For transitional flow, Eq. (3) is combined with Eqs. (4), (6), and (7) to describe water head time oscillations.

For transitional flow, wave parameters (mean water head, amplitude, and frequency) were analytically described as a function of pipe Froude number and dimensionless plunged length. For weir flow, no analytical approach was attempted because of the scarce number of data; interpolation provided a head-discharge relation which resembles the overfall equation. Finally, some benefic effects generated by a venting pipe were noticed: specifically, experiments under unvented conditions, whose results were not reported in this paper, showed that oscillations of water head occurred in such a short time and the water surface was so turbulent that data were considered unreliable.

Notation

The following symbols are used in this paper:

A^* = dimensionless oscillation amplitude = a_{m}/nD (-);
A_{m} = dimensionless oscillation amplitude = $a_{\mathrm{m}}/D_{\mathrm{eq}}$ (-);
a_{m} = oscillation amplitude (m);
D = diameter of drop shaft (m);
D_{eq} = equivalent diameter = $(D^2 - d^2)^{1/2}$ (m);
d = diameter of coaxial pipe (m);
F_D = pipe Froude number = $Q/(gD_{\mathrm{eq}}^5)^{1/2}$ (-);
h = water head over intake section (m);
h_{m} = mean water head over intake section (m);
L = length of drop shaft (m);
L_p = length of pressurized flow region (m);
n = plunging rate of coaxial pipe (-);
Q = discharge ($\mathrm{m^3\,s^{-1}}$);
S_0 = Strouhal number for peak frequency ϕ_0 (-);
$\mathsf{S}_{0\max}$ = Strouhal number for maximum peak frequency $\phi_{0\max}$ (-);
t = time (s);
V = flow velocity ($\mathrm{m\,s^{-1}}$);
Y = dimensionless water head = h/D_{eq} (-);
Y_{m} = mean dimensionless water head = $h_{\mathrm{m}}/D_{\mathrm{eq}}$ (-);
ϕ_0 = oscillation peak frequency (Hz);
$\phi_{0\max}$ = maximum oscillation peak frequency (Hz);
λ = dimensionless length = L/D_{eq} (unvented drop shaft) or = nD/D_{eq} (vented drop shaft) (-); and
μ = discharge coefficient for overfalls (-).

Subscripts

c = computed; and
o = observed.

References

Anderson, A. G., Vaidyaraman, P., and Chu, C. (1971). "Hydraulics of long vertical conduits and associated cavitation." *Water Pollution Control Research Report, Environmental Protection Agency, Rep. No. 122*, St. Anthony Falls Hydraulics Laboratory, Univ. of Minnesota, Minneapolis.

Anwar, H. O. (1965). "Coefficients of discharge for gravity flow into vertical pipes." *J. Hydraul. Res.*, 3(1), 1–19.

Banisoltan, S., Rajaratnam, N., and Zhu, D. Z. (2015). "Experimental study of hydraulics of drill-drop manholes." *J. Hydraul. Eng.*, 10.1061/(ASCE)HY.1943-7900.0001042, 04015021.

Del Giudice, G., and Gisonni, C. (2011). "Vortex dropshaft retrofitting: Case of Naples city (Italy)." *J. Hydraul. Res.*, 49(6), 804–808.

Del Giudice, G., Gisonni, C., and Rasulo, G. (2010). "Design of a scroll vortex inlet for supercritical approach flow." *J. Hydraul. Eng.*, 10.1061/(ASCE)HY.1943-7900.0000249, 837–841.

Hager, W. H. (2010). *Wastewater hydraulics: Theory and practice*, 2nd Ed., Springer, Berlin.

Hager, W. H., and Del Giudice, G. (1998). "Generalized culvert design diagram." *J. Irrig. Drain. Eng.*, 10.1061/(ASCE)0733-9437(1998)124:5(271), 271–274.

Khatsuria, R. M. (2005). *Hydraulics of spillways and energy dissipaters*, Civil and Environmental Engineering, New York.

Padulano, R., Del Giudice, G., and Carravetta, A. (2013). "Experimental analysis of a vertical drop shaft." *Water*, 5(3), 1380–1392.

Padulano, R., Del Giudice, G., and Carravetta, A. (2015). "Flow regimes in a vertical drop shaft with a sharp-edged intake." *J. Appl. Water Eng. Res.*, 3(1), 29–34.

Potter, M. C., Wiggert, D. C., and Ramadan, B. H. (2011). *Mechanics of fluids*, 4th Ed., Cengage Learning, Mason, OH.

USBR. (1987). *Design of small dams*, U.S. Dept. of the Interior, Bureau of Reclamation, Washington, DC.

Williams, O. (1997). *Tunnels and shafts in rock*, CECW-ED, Washington, DC.

J. Irrig. Drain Eng., 2016, 142(5): 06016002